AD_____

Award Number: W81XWH-06-1-0449

TITLE: Early Detection of Breast Cancer via Multi-Plane Correlation Breast Imaging

PRINCIPAL INVESTIGATOR: AMARPREET S. CHAWLA, M.S.
EHSAN SAMEI, Ph.D.

CONTRACTING ORGANIZATION: Duke University Medical Center
Durham, North Carolina 27710

REPORT DATE: April 2009

TYPE OF REPORT: Annual Summary

PREPARED FOR: U.S. Army Medical Research and Material Command
Fort Detrick, Maryland 21702-5012

REPORT DOCUMENTATION PAGE

Form Approved
OMB No. 0704-0188

1. REPORT DATE *(DD-MM-YYYY)*	2. REPORT TYPE	3. DATES COVERED *(From - To)*
01-04-2009	Annual Summary	31 Mar 2006 - 30 Mar 2009

4. TITLE AND SUBTITLE
Early Detection of Breast Cancer via Multi-Plane Correlation Breast Imaging

5a. CONTRACT NUMBER

5b. GRANT NUMBER
W81XWH-06-1-0449

5c. PROGRAM ELEMENT NUMBER

6. AUTHOR(S)
AMARPREET S. CHAWLA

EHSAN SAMEI

Email: asc14@duke.edu

5d. PROJECT NUMBER

5e. TASK NUMBER

5f. WORK UNIT NUMBER

7. PERFORMING ORGANIZATION NAME(S) AND ADDRESS(ES)
Duke University Medical Center

Durham, NC 27705

8. PERFORMING ORGANIZATION REPORT NUMBER

9. SPONSORING / MONITORING AGENCY NAME(S) AND ADDRESS(ES)
U.S. Army Medical Research and Material Command
Fort Detrick, Maryland
21702-5012

10. SPONSOR/MONITOR'S ACRONYM(S)

11. SPONSOR/MONITOR'S REPORT NUMBER(S)

12. DISTRIBUTION / AVAILABILITY STATEMENT
Approved for public release; distribution unlimited

13. SUPPLEMENTARY NOTES

14. ABSTRACT

One major deficiency of standard mammography that limits its accuracy in detecting breast cancer is the camouflaging effect of overlapping structures in the projection images. To minimize this effect, we proposed Multi-plane Correlation Imaging (MCI) technique. In this technique, multiple radiographic images of the breast are obtained from different angles in rapid succession. Angular information is used to identify and positively reinforce the lesion signals between different projections.

In this research work, a theoretical foundation based on mathematical observer model was laid out to model the diagnostic process in MCI. Using this model, a framework was developed to optimize data acquisition in MCI to maximize its diagnostic performance. The framework was then validated using a new CADe processor. Furthermore, it was extended to optimize tomosynthesis and to compare its performance with MCI. The results revealed that the peak performance for MCI at dose levels of single-view mammography was achieved at 15 – 17 projections spanning an angular arc of ~45°, the widest angle tested in this study. An average angular separation of ~2.75° was found to be optimum. Overall, performance of optimized MCI exceeded that of standard mammography by 18% and that of tomosynthesis by 8%. MCI may thus prove to be potentially more accurate, and cost- and dose- effective breast imaging technique.

15. SUBJECT TERMS
Mammography, Tomosynthesis, Multi-projection Imaging, Laguerre-Gauss Channelized Hotelling Observer, ROC, Detectability Index, SKE, Computer Aided Detection (CADe).

16. SECURITY CLASSIFICATION OF:			17. LIMITATION OF ABSTRACT	18. NUMBER OF PAGES	19a. NAME OF RESPONSIBLE PERSON
a. REPORT	b. ABSTRACT	c. THIS PAGE			USAMRMC
U	U	U	UU	30	19b. TELEPHONE NUMBER *(include area code)*

Table of Contents

Page

INTRODUCTION

In the US, breast cancer is the second most common cancer amongst women as well as the second leading cause of death. An estimated 40,460 breast cancer deaths occurred in 2007. [1] Mammographic screening can help detect cancer before it shows symptoms and dramatically increase survival rates. However, the false negative rate of mammographic procedures is in 10-30 % range, thus limiting the effectiveness of mammography in reducing mortality.[2,3-5] At the same time, the false positive rate is estimated to be 11.5 %.[6-8]

In mammography, a 3D volume of anatomical structures is collapsed into a 2D image plane. The resultant image, therefore, is a consequence of projection of overlapping anatomical structures into a complex 2D image. As a result, any abnormality in the form of breast cancer may easily get hidden behind projections of a normal tissue structures, resulting in low sensitivity. At the same time, the overlapping structures may also mimic the pathology that the radiologists are looking for, leading to high rate of false positives. An imaging technique which may alleviate the limiting factor of overlapping anatomical structures and at the same time take advantage of standard mammography imaging technique, may therefore prove to be highly effective in breast cancer screening.

The Proposed System: Multi-plane Correlation Imaging (MCI)

MCI is a realization of multi-projection imaging scheme in which a plurality of digital radiographic images of the same patient is acquired within a short interval of time from slightly different angles. The acquisition protocol is similar to tomosynthesis technique with a difference that the images are directly analyzed instead of reconstructing them, thereby avoiding reconstruction artifacts. These images are similar to projection images acquired in standard projection technique, except that each of the angular projections is acquired with a lower dose level such that the total patient dose is within the bounds of an optimized acquisition. The acquired images are then processed by a combinatorial technique that exploits the differences in geometrical perspectives that different projections offer to establish spatial correlation information between different angular projections. This information is used to identify and positively reinforce the lesion signals between different projections, thus minimizing the fundamental limiting factor imposed by anatomical noise on the detection of lesions. A schematic of MCI and its relationship to tomosynthesis is shown in Fig.1.

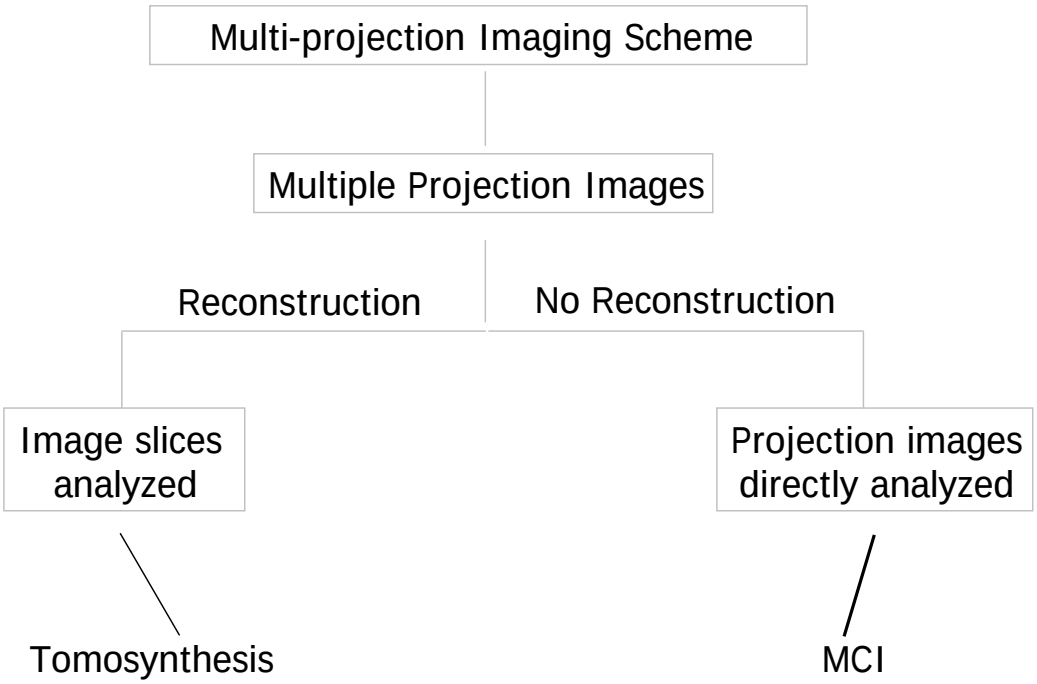

Fig. 1: Schematic of Multi-plane Correlation Imaging (MCI) illustrating its lineage.

Clinical Significance of MCI

MCI meets the unmet need in diagnostic radiology for a technique that enables radiologists to faithfully differentiate cancer from normal tissue and show cancers hidden by superimposition of anatomical structure. When combined with a rapid acquisition digital x-ray detector, MCI may be implemented on modified radiographic imaging systems in a cost-effective way, and incorporated to yield high patient throughput. Practically, MCI can be implemented in different forms including scrolling the images manually or in cine mode, stereoscopic display of projections images, or computer-aided analysis of the images. Overall, if perfected and implemented using optimized data acquisition scheme, MCI could provide a simple and accurate cancer diagnosis over projection imaging techniques at lower patient dose levels.

Compared to tomosynthesis, MCI technique could provide a simpler, faster and lower cost alternative with comparable or better performance for the detection of cancer, potentially at lower dose levels. Furthermore, the absence of the need to reconstruct images, and thus the associated artifacts inherent in tomosynthesis imaging, provides the MCI technique an immediate advantage in terms of the diagnostic image quality. Moreover, as compared to tomosynthesis in which as many as 50–80 slices may need to be reviewed depending on the size of the patient, the MCI technique may entail investigating a significantly fewer number of images, resulting in higher throughput and potentially improved confidence or even accuracy of a radiologist's decision.

We also envision the use of MCI as an adjunct to tomosynthesis imaging, with no added patient dose. The CAD technique developed for MCI may be applied to the projection images acquired in the process of tomosynthesis imaging, providing the radiologist with a second diagnostic opinion. Thus, as with tomosynthesis, besides mammography and chest imaging, MCI could be used in a wide ranging applications including, but not limited to, brachytherapy,[9] hand arthritis,[10] dental,[11] and radiotherapy applications.[12]

Optimization of MCI

In MCI several possible combinations of its data acquisition parameters such as the acquisition dose level, the number of angular acquisitions, and the total angular span of those acquisitions may be used. Not all of these combinations, however, are optimal – certain combination of these parameters may quickly distort pathological indicators, making it important to derive an optimum acquisition scheme that would make MCI maximally effective.

While some initial studies on optimization of tomosynthesis have been conducted they cannot be directly applied to MCI. This is because most of the current optimization protocols are not based on maximizing the quality of output images – which is an important factor in characterizing the clinical utility of a system.[13] The optimization, therefore, should focus on the dependence of imaging system performance on system configuration and derive a specific configuration that delivers best system performance. An optimized data acquisition scheme will yield superior diagnostic accuracy of MCI, particularly important for the early detection of cancer. Furthermore, optimizing acquisition parameters will allow to fully realize the potential of MCI in delivering superior diagnostic performance at a dose level lower than that delivered in standard procedures. This would be in line with the "as low as reasonably achievable" (ALARA) dose principle governing cancer screening.

Proposed Work

In this work, we investigated the feasibility of a new optimized image acquisition and processing approach, namely, Multi-projection Correlation Imaging (MCI). The hypothesis of this study was that the detection of cancer can be improved by minimizing the undesirable influence of overlying anatomical noise by harnessing correlation information between multiple projections of the same patient in an optimized fashion. Grounded on this hypothesis, this research aimed to (a) theoretically demonstrate the clinical advantage in using MCI over standard projection technique as a new diagnostic tool for improved cancer detection, (b) develop and validate a framework to optimize the image acquisition process in MCI, (c) use this framework to establish an optimization rule for MCI and its other multi-projection imaging counterpart, namely tomosynthesis, and finally (d) compare clinical performance of MCI with tomosynthesis to examine its clinical utility.

BODY

Specific Aim 1: Determine the set of acquisition parameters for an MCI study. (Months 1-9)

Progress: Work for this task has been accomplished and was detailed in the last annual report. The goal of this task was to acquire images that approximate mammographic backgrounds which could then be used for analysis in developing methodologies for the other specific aims of this study.

Conclusions of Task 1

Sub-optimized implementation of MCI can potentially compromise its maximum achievable diagnostic performance. In this task, we developed an algorithmic observer-based framework to assess the impact of various acquisition parameters of MCI performance, namely, dose, the number of projections, and the angular span. The study demonstrated the interplay of anatomical and quantum noise in the overall performance. The following conclusions were drawn from this phase of the study:

1) Increasing the number of projections while keeping the overall dose and angular span constant decreased the performance of MCI.
2) Increasing the angular span and acquisition dose level improved the maximum obtainable AUC.
3) The number of projections required to maximize performance was found to be linearly related to the angular span. This number was found to be independent of the acquisition dose level. The best clinical performance was obtained when the angular separation between each projection was approximately 2.75^{o}.
4) Finally, the results revealed that the peak performance for MCI at the clinically relevant dose levels of one- and two-view mammography was achieved at 15 – 17 projections spanning an angular arc of ~45^{o}, the widest angle tested in this study.

The outcome of this task was published in two articles the journal of Medical Physics in 2007 and 2008:

(a) **Chawla A.**, Samei E., Saunders R., Abbey C., Delong D., Effect of dose reduction on the detection of mammographic lesions: A mathematical observer model analysis, *Medical Physics* 34: 3385-3398, 2007.

(b) **Chawla A.**, Samei E., Saunders R., Lo J., Baker J., A mathematical model platform for optimizing a multi-projection breast imaging system, *Medical Physics* 35: 1337-1345, 2008.

Specific Aim 2: Extend single-view CAD processi ng m ethods used for conventional mammography for MCI implementation using a multi-plane correlation rule. (Months 10-21)

Progress: Work for this task has been com pleted as well and was detailed in the last annual report. A CADe processor developed earlier for standard projection technique was extended to take advantage of the MCI configuration.[14]

Conclusions of Task 2

A new CADe processor was developed for multi-projection Correlation Imaging (CI) that takes adv antage of the g eometrical c orrelation in formation a ccrued f rom the ava ilable m ultiple projections to im prove specificity of the CI system. The perfor mance of CADe proc essor was found to be robust as it is successfully able to locate the suspected lesions.

The work resulting from this task was subm itted to the journ al of Academ ic Radiology and has now been accepted for publication. The s ubmitted m anuscript h as been attached in the appendix.

- Cha wla A., Samei E., Lo J.Y, Baker J., Toward Optim ized Acquisition Sche me f or Multi-projection Correlation Imaging of Breast Cancer, In print, Academic Radiology, 2008.

Specific Aim 3: *Fine-tune the optimized formalism of step 1 for CAD algorithm and evaluate its performance.*

Progress: Work for this task has been completed. The optimization results obtained with observer model processor in step 1 were compared and substantiated with those obtained with CADe processor.

Task 3.1: Apply the CAD algorithm on multi-projection images of breast specimens to test the optimality of parameters established in task 1. (Months 22-25)

To meet the goals of this aim, the acquisition parameters were systematically changed and the CADe-based performance measured for different settings of those parameters. These results were compared to the observer model-based performance to confirm the optimality of MCI scheme.

The specific methods developed to accomplish this task will be detailed here.

a. Image Database

The study employed a database of image sets from 106 subjects recruited for our ongoing tomosynthesis clinical trial.[15] Each image set consisted of 25 images of a single breast acquired about the CC or MLO orientation from 25 different but fixed angular positions uniformly spaced in steps of 1.8^{o} over a $\sim 45^{o}$ arc. A prototype clinical multi-projection system, Siemens' Mammomat Novation ^{TOMO} (Fig. 2) was used.[16] The images were acquired at kVps ranging between 28 and 30, with a total glandular dose less than that delivered in a standard two-view screening procedure. All cases were interpreted by one of five dedicated breast imaging radiologists to be normal (without any lesions).

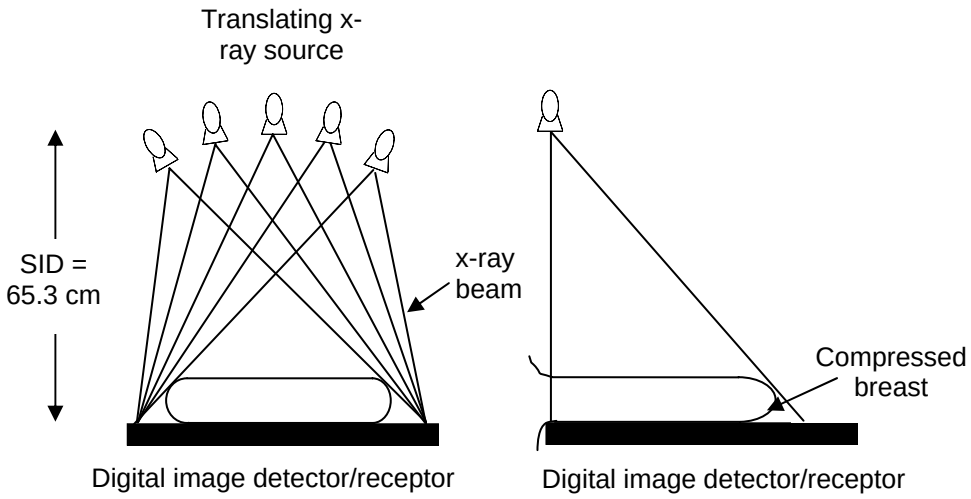

Fig. 2: Schematic of acquisition for multi-projection breast Correlation Imaging (CI). Front view (left); side view (right)

Next, a database of lesion present images was generated. Toward that end, 53 out of the available 106 cases in the database of normal clinical images were supplemented with projections from a simulated 3D 3 mm lesion.[17] The lesion was simulated to be located at the center of the breast a distance of 3 cm above the detector plane. The projections of this lesion on the detector were simulated for all the 25 different tube positions and embedded into corresponding angular projections of the subject images. Thus there were two datasets each of 53 subjects, one with lesion absent and the other with lesion present. The contrast of the lesion was set assuming a heterogeneous breast (50% glandular/50% adipose tissue, representing an average breast composition) and accounting for the acquisition kVp, target/filter combination, breast thickness, anode type, and appropriate scatter fractions.[18]

b. Optimization of Data Acquisition and Comparison with Observer-model Results

To optimize the acquisition scheme, the components of acquisition, namely, the number of projections and their angular span were systematically changed within 2 – 25 and 3.6 ^{o} – 44.8 ^{o} range, respectively, to investigate which one of the many possible combinations yielded the highest diagnostic performance.

Area under the ROC curve (AUC) was derived from the datasets with and without the embedded lesion. Each case in the two datasets was processed with the CADe processor described earlier to yield a corresponding 2D contour map. The likelihood of the presence of the embedded lesion was examined via a correlation matching of the expected signal with the signal-present and with the signal-absent 2D contour map. The value obtained by this signal-matching step served as decision variables based upon which the probability distribution functions (*pdf*) of the signal-absent and signal-present decision variables were computed. Finally, non-parametric ROC curves were derived by thresholding the *pdfs*, and AUC subsequently computed by the trapezoidal method.

AUC was computed using location and signal known exactly (SKE) paradigm similar to the procedure used by mathematical observer model processors. Therefore, although not equivalent, the AUC values obtained by the two processors are comparable. Most importantly, they provide a single platform on which to compare the performance results of observer-model may be compared with those from CAD.

Results of Task 3.1

Fig. 3 shows the variation of AUC with the number of projections spanning different angular arcs. At each angular range, the AUC values increase with the increase in the number of angular projections and then appear to approach an asymptote. The number of projections at which the AUC values peak depends on the angular span. The highest AUC is obtained at the maximum angular span of 44.8^{o} with 7 projections.

The trend in the variation of AUC values delineate the role of different components of acquisition scheme in the final diagnostic performance of a multi-projection imaging system. These trends indicate that the optimum number of projections for a multi-projection imaging system may be in the 7-10 range for an angular span of 44.8 ^{o}. Most noteworthy, the observer model results (reported in the last annual report and reproduced here in Fig. 4 for convenience) show a similar trend in performance where the maximum detectability of an embedded lesion was found to maximize with between 10-17 angular projections for an angular span of 44.8^{o}.

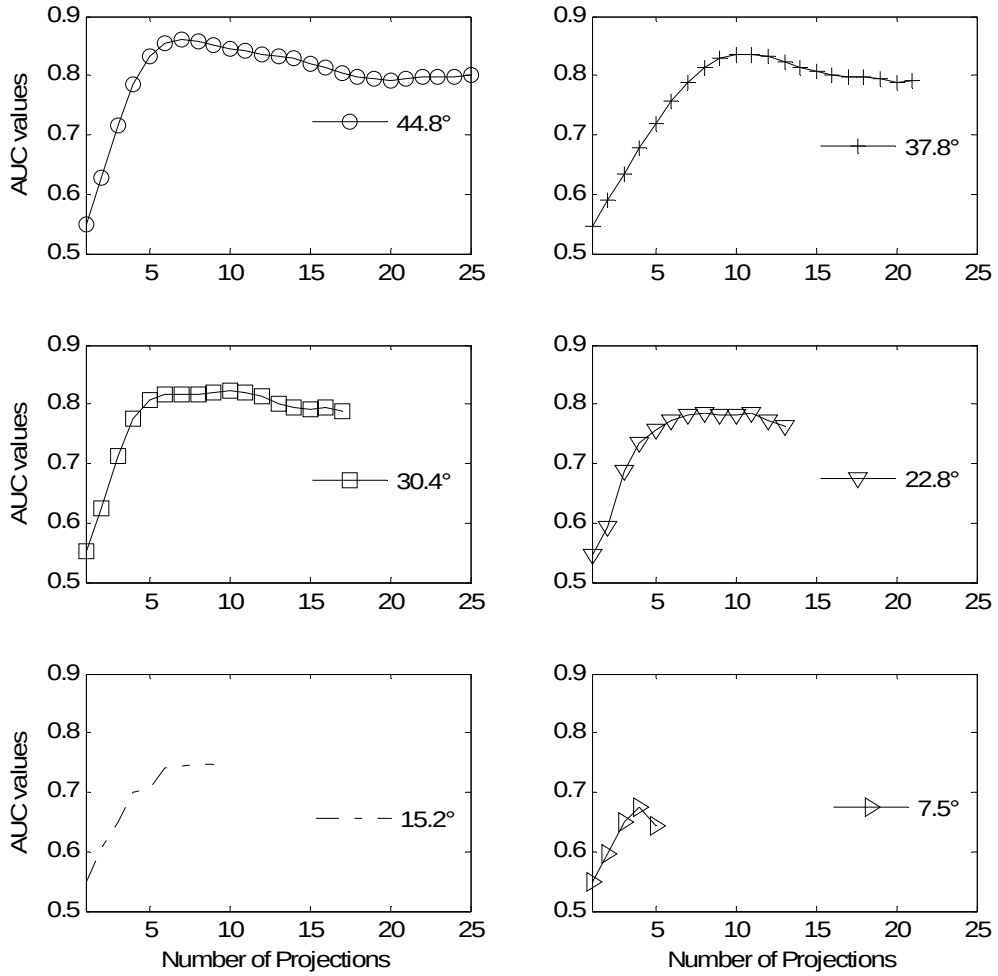

Fig. 3: Area under ROC curves as a function of the number of projections spanning different angular ranges (specific values shown in the legends) in a Multi-plane Correlation Imaging setup. AUCs indicate the detectability of a simulated mass embedded into each projection**.**

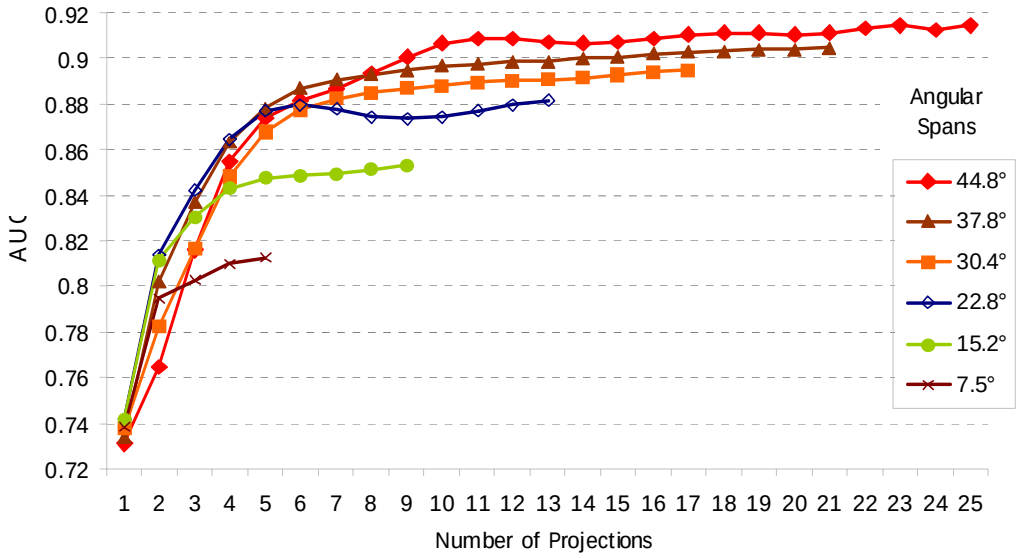

Fig. 4: Variation of AUC for different number of angular projections spanning for representative angular spans in the 7.5°-44.8° range using a mathematical observer model. These results confirm the optimization results obtained from the CADe processor (shown in Fig. 3).

Task 3.2: Compare the detection performance of extended CAD algorithm for MCI with that of an available single-view CAD algorithm used in conventional mammography. (Months 26-28)

This task was accomplished as a part of task 3.1 in which the performance of CADe for MCI was determined at different acquisition settings, including that for single-view conventional mammography. Specifically, the diagnostic performance was measured in terms of two performance indices, first as the ratio: True Positives/(True Positives + False Positives). This ratio, termed Positive Predictive Index (PPI), is a measure of the true positive locations as a fraction of the total number of identified locations per image set and is easily derivable from the FROC curves. These values were then averaged across all the cases for each possible combination of the number of projections and angular range.

Fig. 5 shows the variation in the average positive predictive index (PPI) with the number of projections within 6 angular spans in the 7.5 °–44.8° range. Most noteworthy, at each angular range, the PPI values first increases with increase in the number of projections. This suggests that CADe for MCI outperformed CADe for single-view conventional mammography. The PPI values further increase with increase in the number of projections and then decrease with an increase in the number of projections, maximizing at a value that is dependent on the angular span. The maximum PPI is obtained for 10 projections spanning an angular arc of 44.8°.

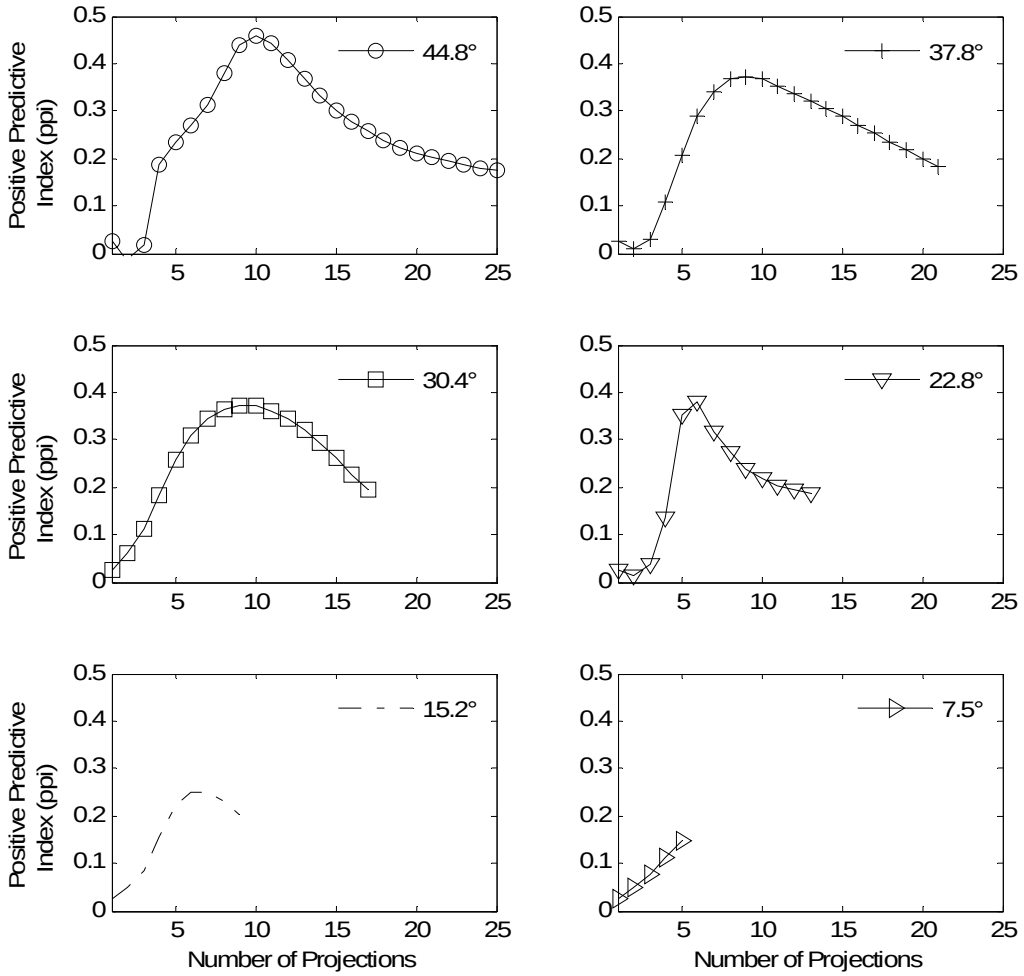

Fig. 5: Average Positive Predictive index [TP/(TP + FP)] as a function of the number of projections spanning different angular ranges (specific values shown in the legends) in a multi-projection Correlation Imaging setup. TP~True Positive findings; FP~ False Positive findings per patient case.

Conclusions of Task 3

In conclusion, the perfor mance of the CADe system was com puted at different data acquisition settings towards optimizing the geometry of image acquisition of MCI. Both the CADe and observer m odel results (reported earlier) show a mutually re inforcing tr ends in th e performance of CI as a function of the differe nt acquisition com ponents, and confirm that the maximum performance may be obtained with 7 –17 projections for an angular span of ~45 ^{o}. Most noteworthy, the optimization framework reported here is based on two se parate clinically-relevant processors and thus could be used to potentially improve the clinical efficiency of MCI.

Specific Aim 4: *Evaluate the clinical performance of MCI and its improvement over the conventional single-view CAD system in the detection of breast cancer using a limited number of human subject cases.*

Work for this task was substituted with a more clinically relevant task of comparing MCI with breast tomosynthesis. This is because breast tomosynthesis is a new breast imaging technique that has shown promising results in improving accuracy of breast cancer detection in recent clinical trials and may possibly receive PMA FDA approval for clinical use in 2009. Thus, to evaluate clinical utility of MCI for eventual clinical adoption, it was paramount to compare its performance to breast tomosynthesis.

Towards meeting the goal of this task, the framework based on projection images reported earlier, was extended to include tomosynthesis reconstruction. The objectives of this task were threefold: (a) to investigate the role of acquistion parameters on the diagnostic quality of breast tomosynthesis at clinically relevant dose levels, (b) to derive a comprehensive optimization rule for tomosynthesis in terms of a specific combination of the acquisition components that renders the best available diagnostic information, and finally, (c) to quantitatively compare the optimized performances of MCI and tomosynthesis.

This task was the major focus of PI's efforts in the last year, and has now been accomplished. The specific methods and framework developed for this phase to meet the goals of this task will be detailed here.

I. Materials and Methods

A. Image database

Images from nice mastectomy specimens that were used in Task 1 to analyze the performance of MCI were employed to investigate the performance of tomosynthesis. To incorporate the specific configuration of tomosynthesis, reconstructed slice volume was generated for each mastectomy specimen. To that end, the projection images with and without supplemented lesions were reconstructed using Siemens' proprietary filtered back projection (FBP)-based reconstruction algorithm, TomoEngine.[19] Variable image slice volumes were generated depending on the compressed size of the specimens to generate fixed slice thickness of 1 mm.

B. Evaluation of Tomosynthesis Detection Performance

For evaluating tomosynthesis, the in-focus slice corresponding to the lesion plane 3 cm above the detector surface was extracted from the reconstructed image slices for each specimen. The specific parameters for reconstruction were dictated by the acquisition configuration considered. The 84 lesion supplemented ROIs/specimen were then extracted from the slice resulting in 756 ROIs for all the specimens. These ROIs were analyzed for the presence of signal using the mathematical model-based methodology similar to that used for CI. At the end of this analysis, a single ROC curve was derived corresponding to the overall detectability of lesions in a reconstructed slice.

C. Optimization Framework

The optimization framework was similar to that used for MCI, except that it was extended to include reconstruction per tomosynthesis configuration. Fig. 6 provides a visual illustration of this multi-factorial optimization scheme. The specific combination of acquisition components that yielded the maximum detection performance was deemed the optimized acquisition parameters set for tomosynthesis.

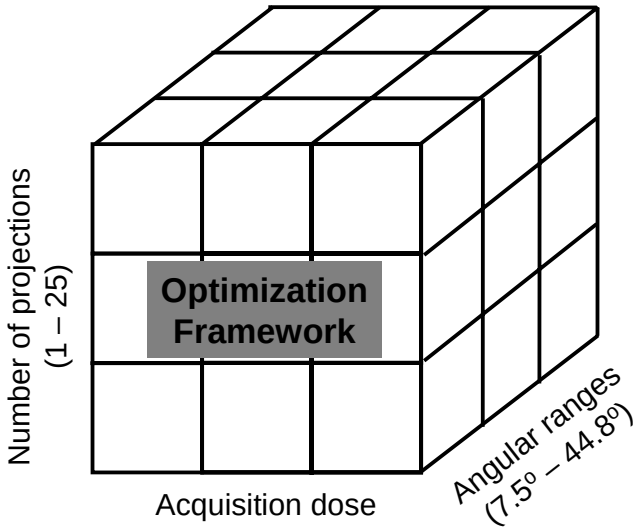

Fig. 6: Schematic of the optimization space used in this study to analyze MCI.

II. Results

Fig. 7 shows variation in AUC with the number of angular projections at different angular ranges for MCI and reconstructed slices (tomosynthesis), respectively, under iso-image dose condition with dose level of each projection was fixed at 1/25 th fraction of typical single-view mammography. (It may be noted that the results for MCI have been reported previously in the last annual report but have been reproduced here for convenience such that a direct comparison of MCI and tomosynthesis may be drawn.)

For both imaging modes, regardless of the angular span, the AUCs first increased with an increase in the number of projections but leveled off beyond a certain number of projections. The maximum value of AUC, however, increased with an increase in the angular span. Projection images yielded a slightly higher maximum AUC than reconstructed slices indicating slight benefit in the detection performance in using just the projection images over tomosynthesis. Most importantly, the peak performance for both imaging modes was between 15 and 20 projections for an angular span of about 45^{o}.

Figs. 8 show reconstructed in-focus slice of a mastectomy specimen under iso-image dose condition of single-view mammography dose level. The slice was generated using 5 (a), 13 (b), and 25 (c) projections spanning a fixed angular range of 44.8^{o}. There is a notable improvement in the detectability of lesions as the number of projections increases from 5 to 13; however, the

detectability does not appear to improve by incr easing the num ber of projections to 25. This provides a visual evidence of the saturation in AUC values shown in Fig. 7b.

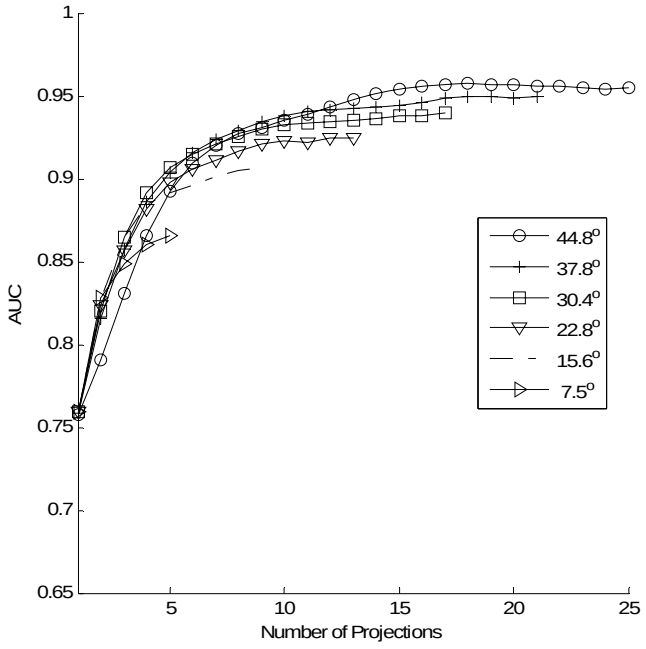

(a)

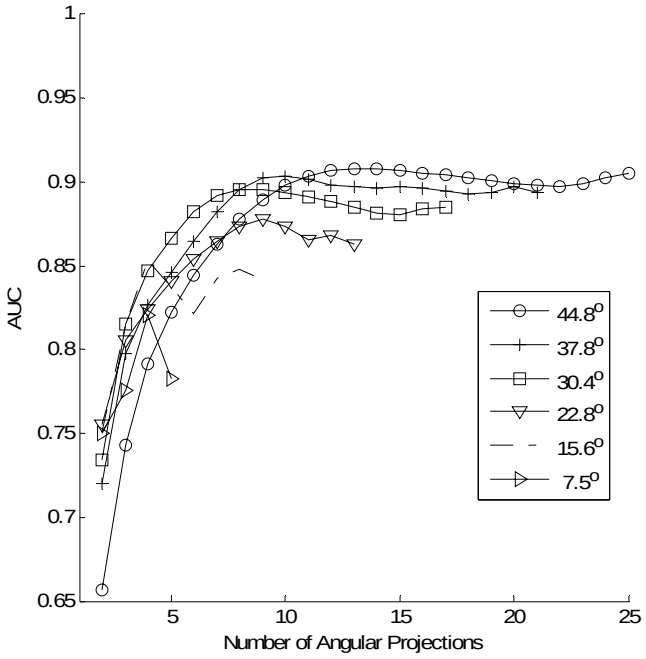

(b)

Fig. 7: Variation of AUC with number of projections for CI (a) and tomosynthesis (b), at different acquisition dose levels under iso-image dose condition (dose of each projection was fixed at 1/25th fraction of typical single-view mammography). The angular spans of these projections were in the 7.5^{o} – 45^{o} range.

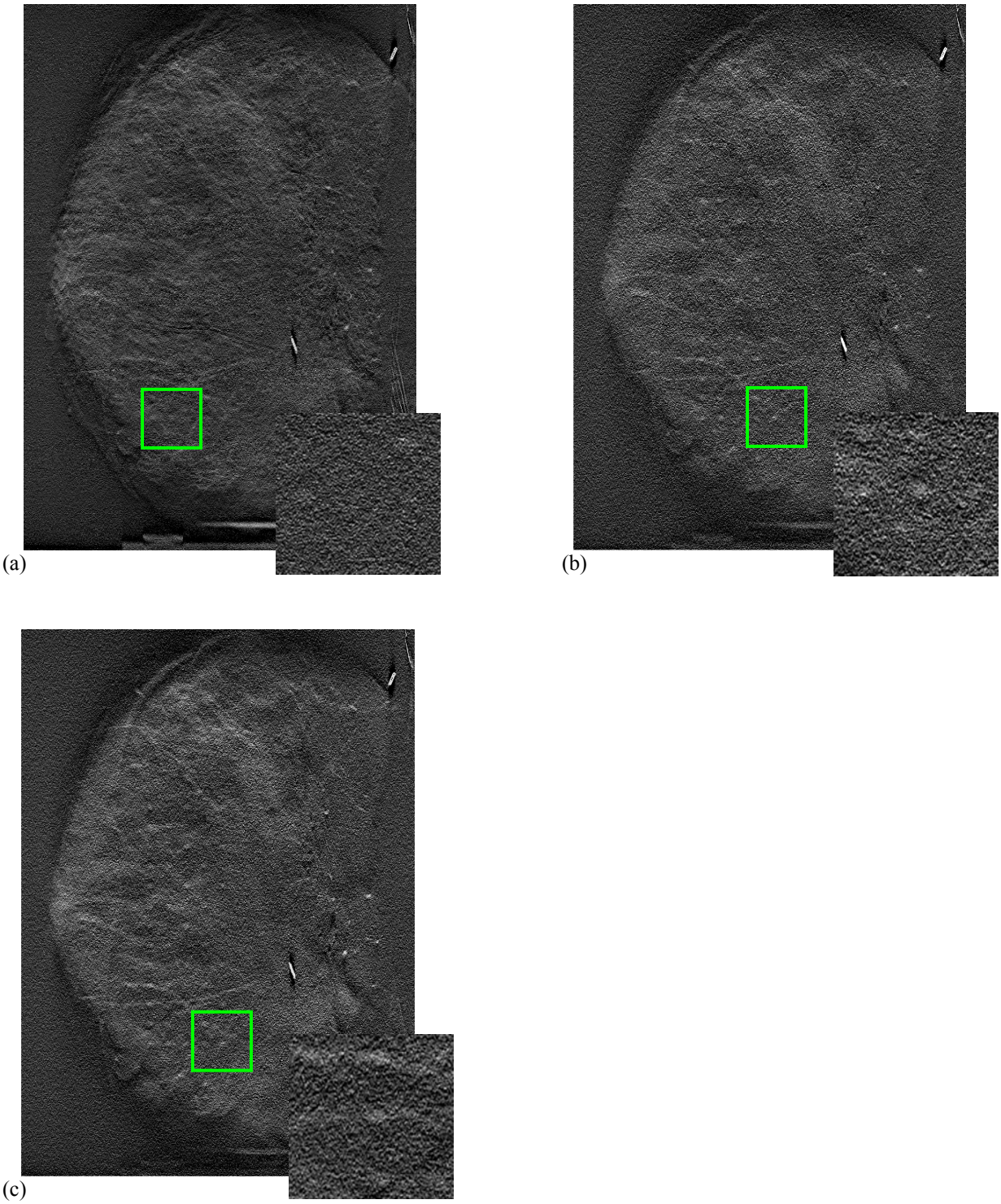

Fig. 8: In-focus tomosynthesis slice at the central plane of lesions embedded in a mastectomy specimen. The slice was reconstructed using 5 (a), 13 (b), and 25 (c) projections under iso-image dose condition (dose of each projection used for reconstruction was fixed at 1/25th fraction of typical single-view mammography). The detectability of the lesion evidently improves from 5 to 13 projections, and then appears to remain steady beyond 13, thus visually confirming saturation in AUC values shown in Fig. 7b.

Figs. 9 and 10 show the variation in AUC with the angular span and number of projection for projection images and reconstructed slices under fixed dose levels (iso-study dose condition) at total dose levels equivalent to that of half and full single-view mammography dose level, respectively. Both projection images and tomosynthesis showed improvement in diagnosis when information from multiple images was combined, confirming the benefit of both methods over standard mammography. However, for all angular spans, the AUC first increased and then decreased as the number of projections was increased. The number of projections at which the AUC values peak was dependent on the angular span. Most noteworthy, the maximum AUC value for both projection images and reconstructed slices was obtained at an angular span of 44.8^{o} with 15 – 17 projections. This suggests that current implementations of breast tomosynthesis with 25 projections may be sub-optimal. Reconstructed slices were also noted to have slightly lower performance than projection images, especially at the half single-view mammography dose level (shown in Fig. 9b), possibly due to reconstruction artifacts that limit the efficiency of tomosynthesis. The higher performance of projection images is thus potentially indicative of the maximum achievable performance via tomosynthesis.

Fig. 11 provides a visual evidence of change in detectability of the embedded lesions in the central slice under iso-study dose condition at dose levels equivalent to that of single- and two-view mammography, respectively. The number of angular projections used to reconstruct the slice was varied from 5 (a) to 13 (b) to 25 (c) spanning a fixed angular arc of 44.8^{o}. At both the dose levels, the detectability of the lesions evidently improved from 5 to 13 projections but decreased when the number of projections was increased to 25.

Figs. 12 and 13 depict that finding for projection images and tomosynthesis. Fig. 12 shows the number of projections that yield maximum AUC at different angular ranges, while Fig. 13 shows the corresponding AUCs at each of those angular ranges. The maximum AUC is obtained using a 44.8^{o} angular span and 15 – 17 projections. As 44.8^{o} was the maximum angular span tested in this study, it is expected that a wider angular span might yield even higher performance. The slope of the linear fit in Fig. 12 reveals that for projection images and reconstructed slices, the optimum angular separation that realizes maximum performance is approximately 2.75^{o}.

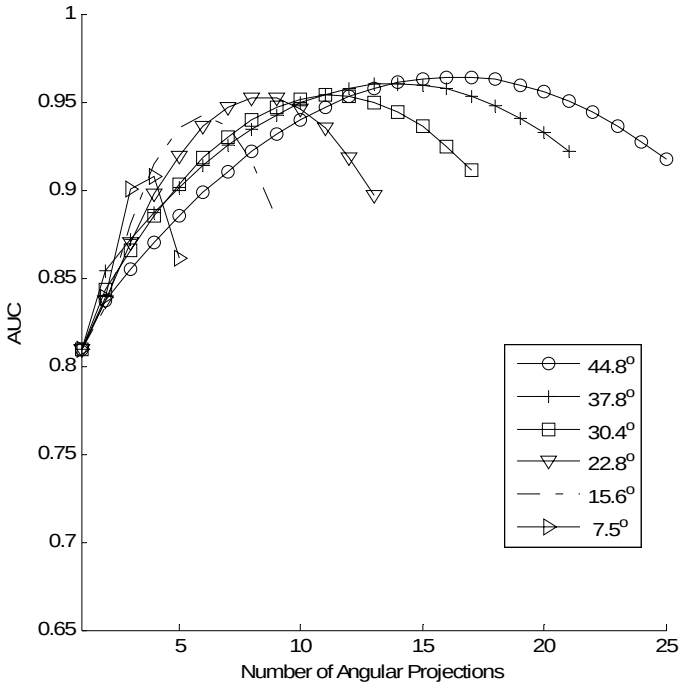

(a)

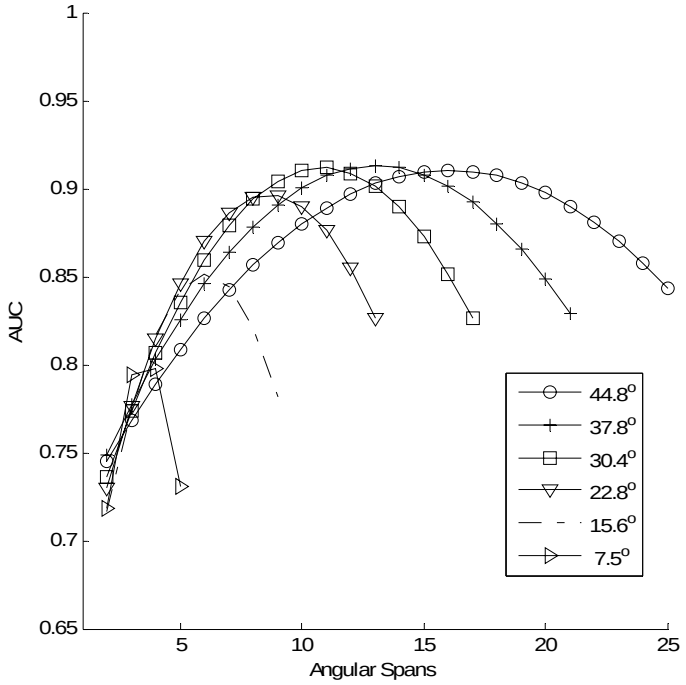

(b)

Fig. 9: Variation of AUC with the number of projections for projections images (a) and reconstructed slices (b) under iso-study dose conditions at different angular ranges in 7.5° - 45° range. The total dose level was fixed to half that of single-view mammography.

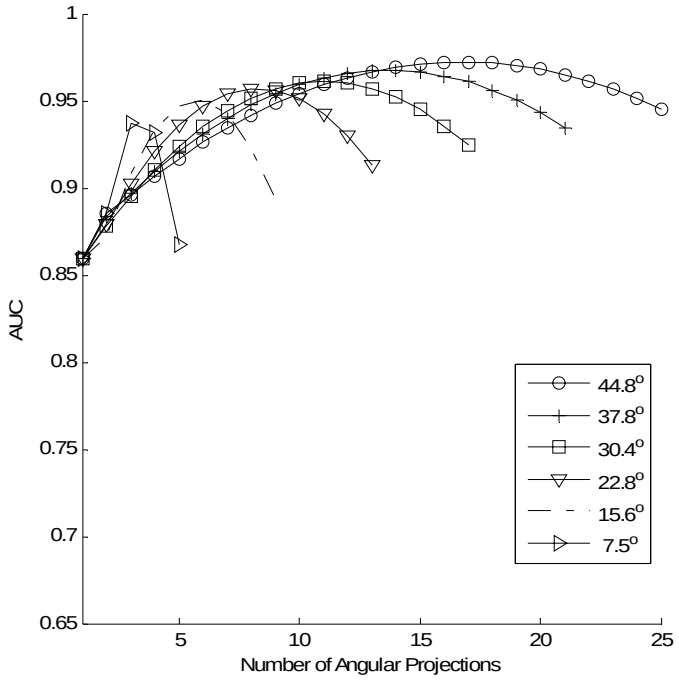

(a)

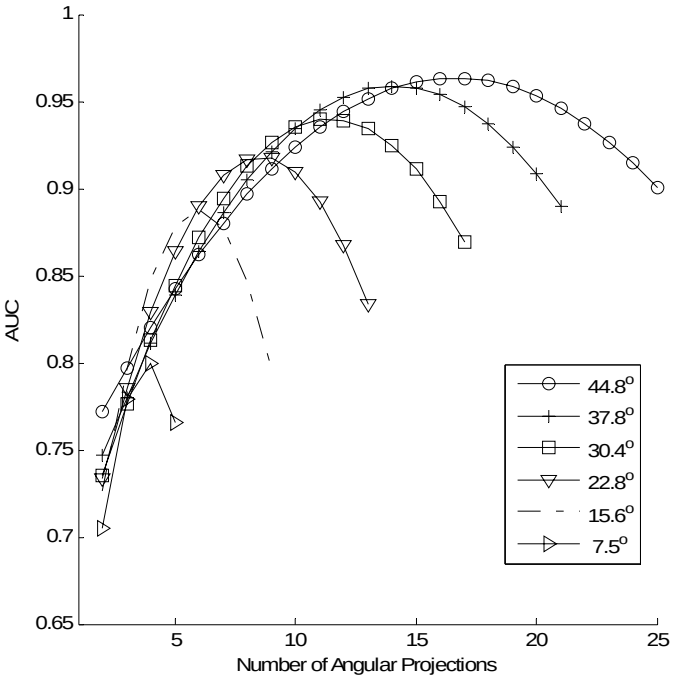

(b)

Fig. 10: Variation of AUC with the number of projections for projection images (a) and reconstructed slices (b) under iso-study dose conditions at different angular ranges in 7.5° - 45° range. The total dose level was fixed to that of single-view mammography.

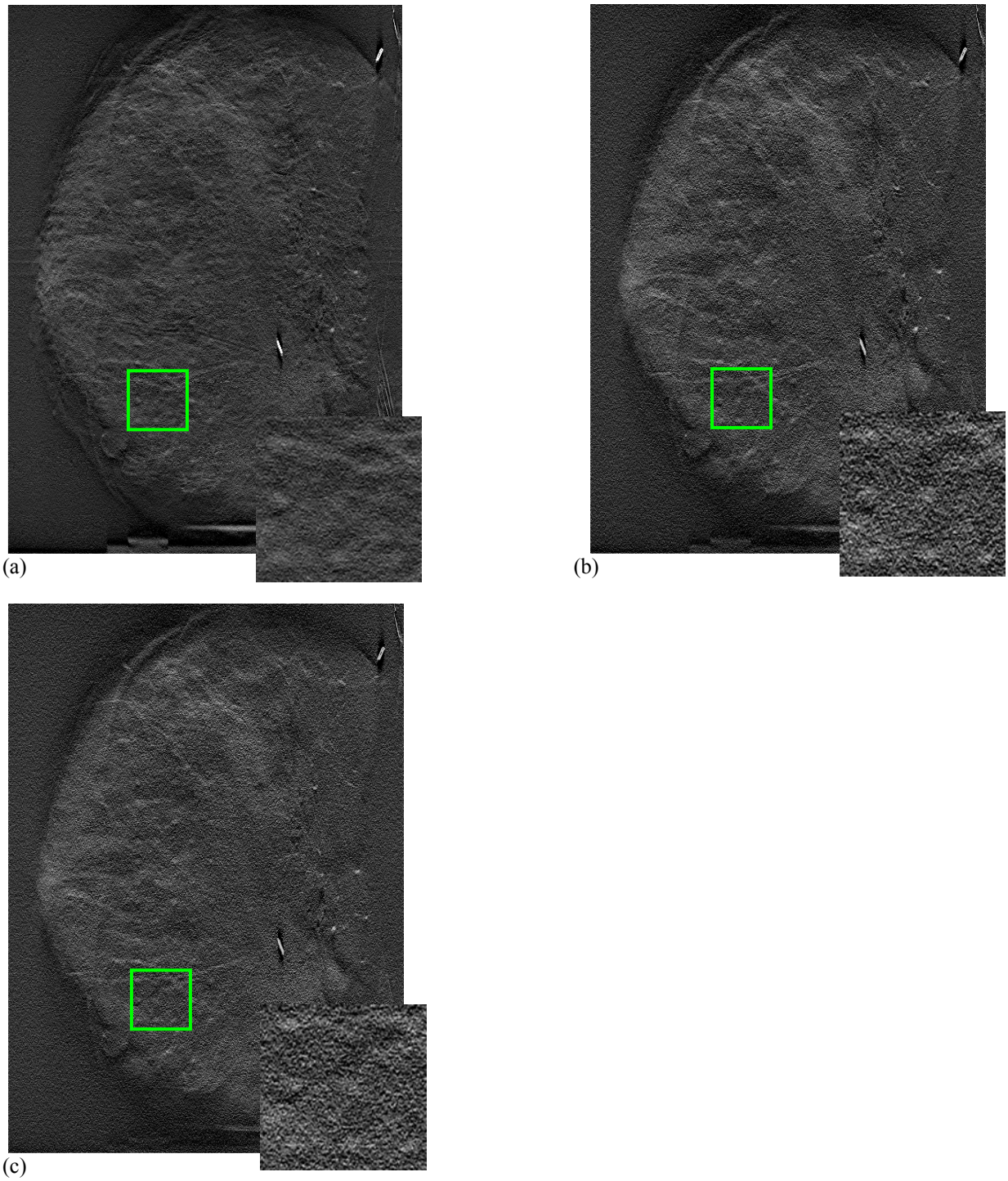

Fig. 11: In-focus tomosynthesis slice at the central plane of lesions embedded in a mastectomy specimen. The slice was reconstructed using 5 (a), 13 (b), and 25 (c) projections. The total dose was fixed at that of single-view mammography regardless of the number of projections. The detectability of the lesion evidently improves from 5 to 13 projections, and then appears to deteriorate at 25 projections due to increased noise per projection, thus visually confirming the roll off in the AUC values shown in Fig. 10b.

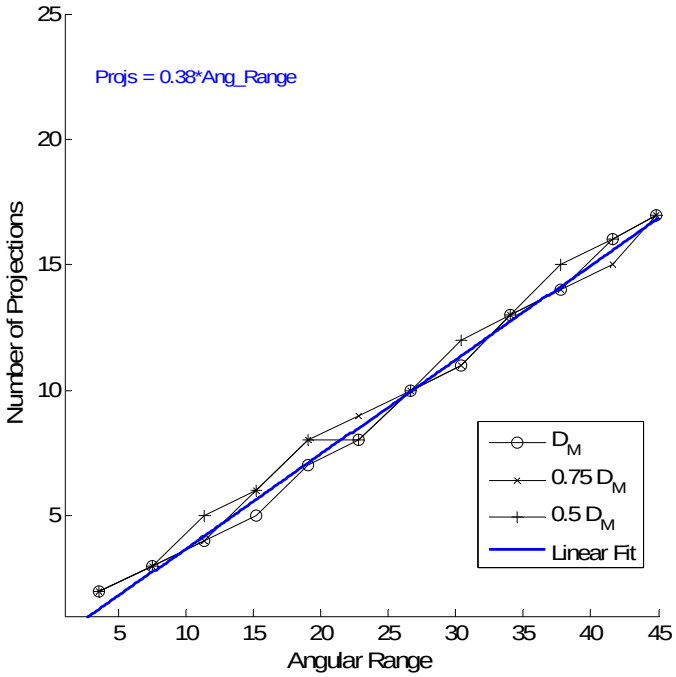

(a)

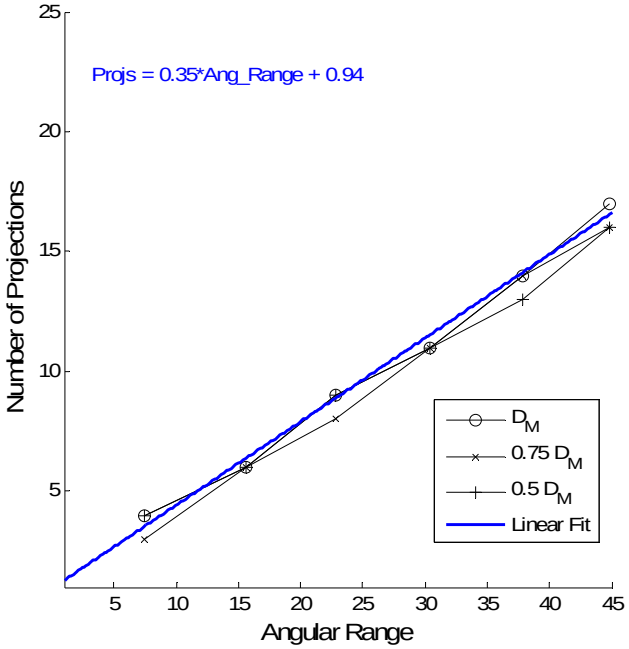

(b)

Fig. 12: The number of projections per angular range that yield maximum AUCs for projection images (a) and reconstructed slices (b). These are plotted for different dose levels (denoted n the legends as the multiples of that of single-view mammography).

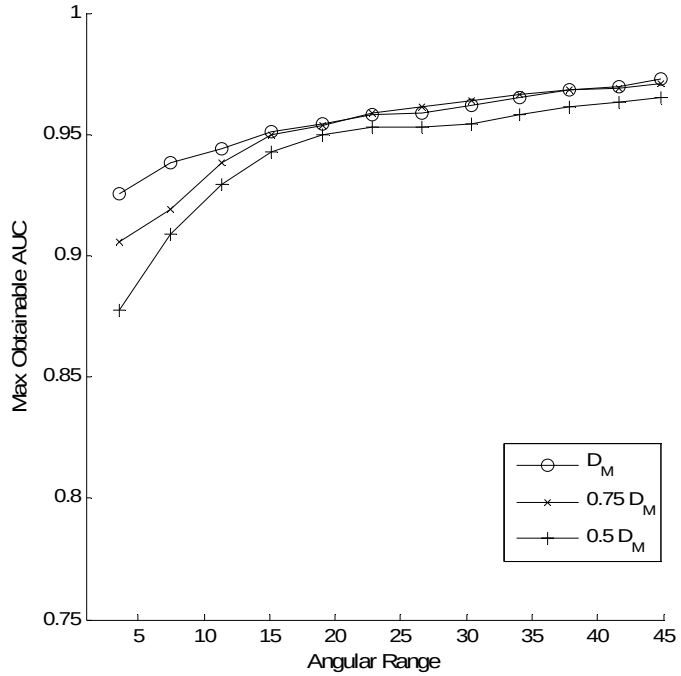

(a)

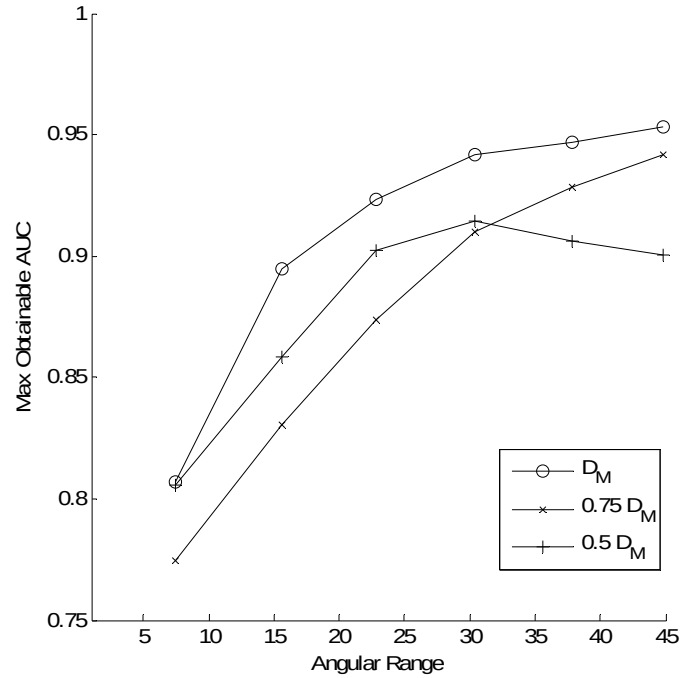

(b)

Fig. 13: Maximum obtainable AUC values for different angular ranges for projection images (a) and reconstructed slices (b). These are plotted for different dose levels (denoted in the legends as the multiple of that of single-view mammography).

KEY RESEARCH ACCOMPLISHMENTS IN YEAR 2006-09

In this research work, we assessed the feasibility of MCI technique, investigated its optimization for maximum diagnostic output, and finally demonstrated its utility for improved breast cancer detection.

Three of the four specific aims outlined in this study were successfully met. The final goal of limited MCI clinical trial was substituted for a more important task of comparing the clinical performance of MCI with that of tomosynthesis. Such a comparison was considered critical since it would have a bearing on establishing clinical utility and thus, ultimately, potential clinical adoption of MCI.

More specifically, in this study, a theoretical model was first developed to determine the diagnostic information content of projection images in MCI using a mathematical observer. Using this model, a multi-factorial task-based framework was developed to optimize the image acquisition of MCI using existing low-dose clinical data. The framework was further validated using a CADe processor. Performance of MCI was evaluated on mastectomy specimens at clinically relevant doses and further compared to tomosynthesis.

Application of the theoretical model on low-dose clinical data showed that peak MCI performance may be obtained with 15-17 projections. CAD results confirmed similar trends. Mastectomy specimen results at higher dose revealed that for both MCI and tomosynthesis, highest dose setting and maximum angular span with an angular separation of 2.75 ^{o} may be optimum, indicating a threshold in the number of projections per angular span for optimum performance. Most importantly, the study demonstrated that the performance of optimized breast MCI may exceed that of mammography and tomosynthesis by 18% and 8%, respectively.

REPORTABLE OUTCOMES

This work resulted in the following journal articles and conference proceedings. The names of the fellow (**Chawla**) and mentor (**Samei**) are boldfaced for emphasis.

Refereed Journal Publications (Attached in the Appendix):

1. **Chawla A**., Lo J.Y, Baker J., **Samei E**., Optimized Image Acquisition for Breast Tomosynthesis in Projection and Reconstruction Space, Submitted for publication in Medical Physics, 2008.
2. **Chawla A., Samei E.,** Lo J.Y, Baker J., Toward Optimized Acquisition Scheme for Multi-projection Correlation Imaging of Breast Cancer, In print, Academic Radiology, 2008.
3. **Chawla A.**, **Samei E.**, Saunders R., Lo J., Baker J., A mathematical model platform for optimizing a multi-projection breast imaging system, *Medical Physics* 35: 1337-1345, 2008.
4. **Chawla A.**, **Samei E.**, Saunders R., Abbey C., Delong D., Effect of dose reduction on the detection of mammographic lesions: A mathematical observer model analysis, *Medical Physics* 34: 3385-3398, 2007.

Conference Proceedings:

5. **Chawla A.**, **Samei E**., Lo J.Y., Mertelmeier T., Multi-projection Correlation Imaging as a new Diagnostic Tool for Improved Breast Cancer Detection, *Proc. IWDM IX*: 635-642, 2008.
6. **Chawla A., Samei E.**, Saunders R.S., Lo J.Y., and Singh S., Optimized acquisition scheme for multi-projection correlation imaging of breast cancer, *Proc. SPIE Medical Imaging* 6915, 691528: 1-8, 2008.
7. Singh S., Tourassi G.D., **Chawla A.**, Saunders R.S., **Samei E**., Lo J.Y., Computer-aided detection of breast masses in tomosynthesis reconstructed volumes using information-theoretic similarity measures**,** *Proc. SPIE Medical Imaging* 6915**,** 691505:1-8, 2008.
8. **Chawla A**., **Samei E.**, and Abbey C., A mathematical model approach toward combining information from multiple image projections of the same patient, *Proc. SPIE Medical Imaging* 6510(1K): 1-11, 2007.
9. **Chawla A.,** Saunders R., Abbey C., Delong D., **Samei E**., Analyzing the effect of dose reduction on the detection of mammographic lesions using mathematical observer models, *Proc. SPIE Medical Imaging* 6146(0I): 1-12, 2006.

OVERALL CONCLUSIONS

In this study, an optimization framework was developed to maximize the diagnostic performance of MCI. It was revealed that the peak performance for MCI at the clinically relevant dose levels of one- and two-view mammography may be achieved at 15 – 17 projections spanning an angular arc of ~45 ^{o}, the widest angle tested in this study. Most importantly, we demonstrated feasibility of multi-plane correlation imaging (MCI) as a technique for improved breast cancer detection. Compared to mammography and tomosynthesis, MCI was shown to be potentially more accurate, and cost- and dose- effective. This study thus paves way for future clinical implementation of MCI.

REFERENCES

[1] American Cancer Society, http://www.cancer.org/. *Cancer Facts and Figures*, (Atlanta, GA, 2007).

[2] R. E. Bird, T. W. Wallace and B. C. Yankaskas, "Analysis of cancers missed at screening mammography," Radiology **184**, 613–617 (1992).

[3] D. B. Kopans, "The positive predictive value of mammography," American Journal of Roentgenology **158**, 521-526 (1991).

[4] D. D. Adler and M. A. Helvie, "Mammographic biopsy recommendations," Current Opinion in Radiology **4**, 123-129 (1992).

[5] H. P. Chan, S. C. Lo, B. Sahiner, K. L. Lam and M. A. Helvie, "Computer-aided detection of mammographic microcalcifications: pattern recognition with an artificial neural network," Medical Physics **22**, 1555-1567 (1995).

[6] L. Tabar and P. B. Dean, "The Control of Breast Cancer through Mammography Screening," Radiologic Clinics of North America **25**, 993-1005 (1987).

[7] E. W. Humphrey, H. B. Ward and R. T. Perri, American Cancer Society, *Clinical Oncology*, Atlanta, GA, second edition, 1995).

[8] J. R. Muhm, W. E. Miller, R. S. Fontana, D. R. Sanderson and M. A. Uhlenhopp, "Lung cancer detected during a screening program using four-month chest radiographs," Radiology **148**, 561-565 (1983).

[9] I. Tutar, R. Managuli and V. Shamdasani, "Tomosynthesis-based localization of radioactive seeds in prostate brachytheraphy," Med. Phys. **30**, 3135–3142 (2003).

[10] J. Duryea, J. Dobbins and J. Lynch, "Digital tomosynthesis of hand joints for arthritis assessment," Med. Phys. **30**, 325–333 (2003).

[11] M. Abreu, D. Tyndall and J. Ludlow, "Effect of angular disparity of basis images and projection geometry on caries detection using tuned-aperture computed tomography," Oral Surgery, Oral Medicine, Oral Pathology, Oral Radiology & Endodontics **92**, 353 - 360

[12] R. D. Zwicker and N. A. Atari, "Transverse tomosynthesis on a digital simulator," Med. Phys. **24**, 867–871 (1997).

[13] T. Wu, R. H. Moore and D. B. Kopans, "Voting strategy for artifact reduction in digital breast tomosynthesis " Med. Phys. **33**, 2461 (2006).

[14] R. S. Saunders, E. Samei, N. Majdi-Nasab and J. Y. Lo, "Initial human subject results for breast bi-plane correlation imaging technique," Proc. SPIE **6514**, 1-7 (2007).

[15] S. Singh, G. D. Tourassi, A. S. Chawla, et al., "Computer-aided detection of breast masses in tomosynthesis reconstructed volumes using information-theoretic similarity measures," Proc. SPIE **6915**, 1-8 (2008).

[16] M. Bissonnette, M. Hansroul, E. Masson, et al ., "Digital breast to mosynthesis using an am orphous selenium flat panel detector," Proc. SPIE **5745**, 529-540 (2005).

[17] A. Chawla, E. Samei, R. Saunders, J. Lo and J. Baker, "A mathematical model platform for optimizing a multi-projection breast imaging system," Med. Phys. **35**, 1337–1345 (2008).

[18] R. S. Saunders, E. Sa mei and C. Hoeschen, "I mpact of resolution and noise charact eristics of digital radiographic detectors on the detectability of lung nodules," Med. Phys. **31**, 1603-1613 (2004).

[19] T. Mertel meier, J. Orman, W. Haerer and M. K. Dudam , "Optim izing filtered backprojection reconstruction for a breast tom osynthesis prototy pe device," Proc. SPIE **6142**, 614 20F61421-61412 (2006).

APPENDIX